

EXTRACTING MECHANICAL PROPERTIES USING REVERSE ANALYSIS OF SINGLE AND DUAL SHARP INDENTATION

M. Dao, N. Chollacoop and S. Suresh

Department of Materials Science and Engineering, Massachusetts Institute of Technology, Cambridge, MA 02139, USA

ABSTRACT

Using dimensional analysis, a set of closed-form dimensionless functions can be constructed to characterize single indenter response. From these functions and finite element computations, analytical expressions were obtained to relate indentation data to elasto-plastic properties. Forward and reverse analysis algorithms were established, where the reverse algorithm allows for the extraction of elasto-plastic properties from a set of indentation data. The proposed reverse algorithm provides a unique solution of the reduced Young's modulus E^* , a representative stress σ_r , and the hardness p_{ave} . This analysis also provides a unique value of σ_y and n for the majority of cases considered. Assuming power law hardening, the full stress-strain response can be readily constructed. A representative stress σ_r was identified at 3.3% plastic strain for a Berkovich (or Vickers, or equivalent cone with 70.3° half-angle) indenter as a strain level which enables a dimensionless description of indentation loading response independent of strain hardening exponent n . Within the same theoretical framework, the underlying consistency between the value of 3.3% found in this study and the values of 8% and 29% proposed in the literature was established, indicating that the apparent disparities are from the differences in functional definitions, rather than from any intrinsic differences in mechanistic interpretations. Additional dimensionless functions were constructed for different indenter tip geometries (i.e., with 50, 60 and 80 degree equivalent cone angles). Adding the 60-degree tip results in the single-indenter algorithm, an improved reverse algorithm for dual indentation was formulated. This dual-indenter reverse algorithm provides a unique solution of the reduced Young's modulus E^* , the hardness p_{ave} and two representative stresses, which allows for uniquely constructing the power-law plastic material response. Experimental verifications were successfully done for two materials.

1 INTRODUCTION

Since Tabor [1] published his classical book on indentation in 1951, significant progresses have been made on instrumented indentation both experimentally and theoretically (e.g., [2-15]). Methods to extract material properties from instrumented indentation response have been investigated in a number of studies (e.g., [1, 4, 7, 14-17, 19-24]). Hill *et al.* [5] first developed a self-similar solution for spherical indentation of a power law plastic material. Extending such an approach to sharp (Berkovich and Vickers) indentation, elastic-plastic analyses of Berkovich and Vickers indentation have been reported within the context of small-strain finite element simulations ([19, 20]). With the application of dimensional analysis to the computational results of large deformation sharp indentation, correlations between elasto-plastic properties and indentation response have also been proposed for bulk [16, 17, 19, 20, 23] and coated [24] material systems. Recently, new methods involving two or more indenters [24-26] were proposed that were shown to significantly improve the accuracy of the reverse analysis.

2 DIMENSIONAL ANALYSIS AND UNIVERSAL DIMENSIONLESS FUNCTIONS

The load (P) versus displacement (h) response of an elasto-plastic material to instrumented sharp indentation can often be described by

$$P = Ch^2 \quad (1)$$

where C is the loading curvature. At the maximum depth h_m , the indentation load P_m makes a projected contact area of A_m . The average contact pressure is thus defined as $p_{ave} = P_m/A_m$, commonly referred as the hardness of the indented material. Upon unloading, the initial unloading slope is defined as $(dP_u/dh)|_{h_m}$, where P_u is the unloading force. After the complete unloading, the residual depth is h_r . The total area under the loading curve is defined as the total work W_t ; the area under the unloading curve is defined as the recovered elastic work W_e ; and their difference is defined as the residual plastic work $W_p = W_t - W_e$. The elasticity follows Hook's law, whereas the plasticity follows Von Mises yield criterion. True stress (σ) and true strain (ε) are related via

$$\sigma = \begin{cases} E\varepsilon, & \text{for } \sigma \leq \sigma_y \\ R\varepsilon^n, & \text{for } \sigma \geq \sigma_y \end{cases} \quad (2)$$

where E is the Young's modulus, R a strength coefficient, n the strain hardening exponent and σ_y the initial yield stress at zero offset strain. In the plastic region, true strain can be further decomposed to strain at yield and true plastic strain: $\varepsilon = \varepsilon_y + \varepsilon_p$.

For a sharp indenter of apex angle θ , the load required to penetrate into a power law elasto-plastic solid (E , ν , σ_y and n) can be written as

$$P = P(h, E^*, \sigma_y, n, \theta), \quad (3)$$

where

$$E^* = \left[\frac{1-\nu^2}{E} + \frac{1-\nu_i^2}{E_i} \right]^{-1} \quad (4)$$

is the reduced Young's modulus, commonly introduced [27] to include elasticity effect (E_i , ν_i) of an elastic indenter. Define σ_r as the stress at the representative plastic strain ε_r , eq. (3) can be rewritten as

$$P = P(h, E^*, \sigma_r, n, \theta) \quad (5)$$

Using dimensional analysis [23, 24], eq. (5) becomes

$$P = \sigma_r h^2 \Pi_{1\theta} \left(\frac{E^*}{\sigma_r}, n, \theta \right), \quad (6a)$$

and from eq. (1),

$$C = \frac{P}{h^2} = \sigma_r \Pi_{1\theta} \left(\frac{E^*}{\sigma_r}, n, \theta \right), \quad (6b)$$

where $\Pi_{1\theta}$ is a dimensionless function. Careful computational studies showed that when a proper representative strain $\varepsilon_r(\theta)$ is chosen [23, 24], eq. (6b) can be expressed independent of hardening exponent n , *i.e.*

$$C = \frac{P}{h^2} = \sigma_r \Pi_{1\theta} \left(\frac{E^*}{\sigma_r}, \theta \right) \quad (6c)$$

Fig. 1 shows the function of $\varepsilon_r(\theta)$ between 50° and 80° degrees. Particularly, at 70.3° (Berkovich and Vickers equivalent) ε_r was identified at 3.3% plastic strain [23], and at 60° ε_r was identified at 5.7% plastic strain [24]. Two additional dimensionless functions Π_2 and Π_3 are also identified for a Berkovich (or Vickers, or a 70.3° equivalent cone) indenter by the following equations [23]:

$$\left. \frac{dP_u}{dh} \right|_{h=h_m} = E^* h_m \Pi_2 \left(\frac{E^*}{\sigma_r}, n \right) \quad (7)$$

and

$$\frac{h_r}{h_m} = \Pi_3 \left(\frac{\sigma_r}{E^*}, n \right) \quad (8)$$

Thus, the three universal dimensionless functions, $\Pi_{1\theta}$, Π_2 and Π_3 , can be used to relate the indentation response to mechanical properties. For complete developments of these functions and the full listings of the closed-form formulae, please refer to [23, 24].

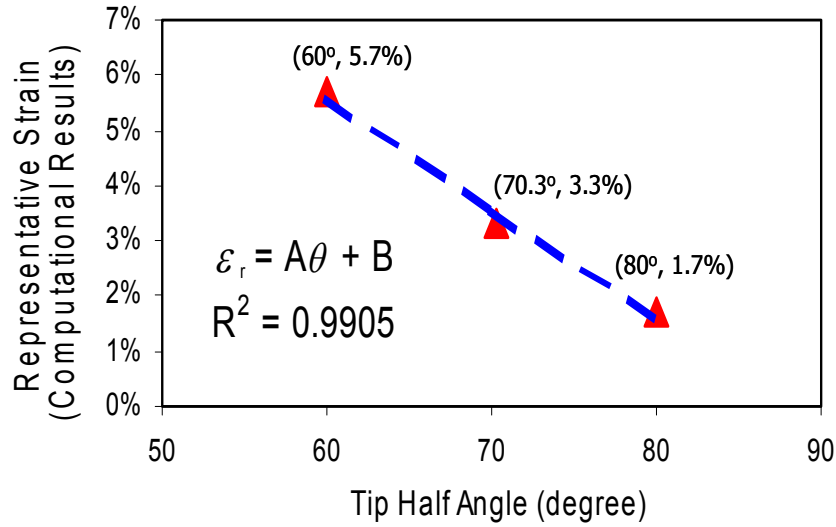


Figure 1. The representative strain as a function of the indenter apex angle [24].

3 SINGLE INDENTER REVERSE ANALYSIS

With a complete set of universal dimensionless functions for a single indenter established, a complete reverse algorithm was constructed for instrumented sharp indentation with an apex angle of 70.3° (Berkovich and Vickers equivalent) [23]. Experimental verifications of the single-indenter algorithm were carried out for two materials: 6061-T6511 and 7075-T651 aluminum alloys [23]. With a set of six tests for an Al 6061-T6511 sample, the reduced Young's modulus E^* was extracted within $\pm 6.5\%$ standard deviation, $\sigma_{0.033}$ within $\pm 3.6\%$, σ_y within $\pm 30.9\%$, and p_{ave} within $\pm 15.9\%$. With a set of six tests for an Al 7075-T651 sample, the reduced Young's modulus was extracted within $\pm 3.0\%$ standard deviation, $\sigma_{0.033}$ within $\pm 5.2\%$, σ_y within $\pm 5.3\%$, and p_{ave} within $\pm 4.9\%$. The proposed reverse algorithm provides a unique solution of the reduced Young's modulus E^* , a representative stress σ_r , and the hardness p_{ave} . This analysis also provides a unique value of σ_y and n for the majority of cases considered. Assuming power law hardening, the full stress-strain response can be readily constructed.

4 DUAL INDENTER REVERSE ANALYSIS

Adding the $\Pi_{1\theta}$ function at 60° to the single indenter algorithm, a new dual-indenter reverse analysis algorithm was established [24]. Experimental verifications of the dual-indenter algorithm were also carried out for two materials: 6061-T6511 and 7075-T651 aluminum alloys [24]. For Al 6061-T6511, the reduced Young's modulus E^* was extracted within $\pm 6.5\%$ standard deviation, $\sigma_{0.033}$ within $\pm 3.6\%$, $\sigma_{0.057}$ within $\pm 1.0\%$, and σ_y within $\pm 16.6\%$; note that with the same set of Berkovich indentation curves, σ_y was extracted using the single-indenter algorithm within $\pm 30.9\%$ standard deviation, which is significantly worse than the dual-indentation results. For Al 7075-T6511, the reduced Young's modulus E^* was extracted within $\pm 8.3\%$ standard deviation, $\sigma_{0.033}$ within $\pm 11.4\%$, $\sigma_{0.057}$ within $\pm 10.4\%$, and σ_y within $\pm 18.7\%$; note that with the same set of Berkovich indentation curves, σ_y was extracted using the single-indenter algorithm within $\pm 38.4\%$ standard deviation, which is again significantly worse than the dual-indentation results. This dual-indenter reverse algorithm provides a unique solution of the reduced Young's modulus E^* , the hardness p_{ave} and two representative stresses, which allows for uniquely constructing the power-law plastic material response.

5 DISCUSSIONS

The concept of representative strain was first introduced by Tabor [1] to relate its corresponding representative stress to the hardness value. Tabor [1] suggested a representative plastic strain of 8-10% based on his experimental observations. Giannakopoulos *et al.* [11] and Giannakopoulos and Suresh [19] used a "characteristic strain" of 29-30%. In our current study [23], a representative plastic strain $\varepsilon_r = 0.033$ at $\theta = 70.3^\circ$ (Berkovich or Vickers equivalent) was identified as a strain level which allows for the construction of a dimensionless description of the indentation loading response (*i.e.*, eq. (6c)), independent of strain hardening exponent n .

As discussed in detail in our recent study [23], within the same elasto-plastic theoretical framework for instrumented sharp indentation, the underlying consistency between the value of 3.3% found in our study and the values of 8% and 29% proposed in the literature can be readily established, indicating that the apparent disparities are from the differences in terms of functional definitions, rather than from any intrinsic differences in terms of mechanistic interpretations.

ACKNOWLEDGEMENTS

This research was supported by the Defense University Research Initiative on Nano-Technology (DURINT) funded at MIT by the Office of Naval Research, Grant No. N00014-01-1-0808 and by a subcontract to MIT through the Center for Thermal Spray Research at Stony Brook, under the National Science Foundation Grant DMR-0080021.

REFERENCES

1. Tabor, D., 1951, *Hardness of Metals*, Clarendon Press, Oxford.
2. Tabor, D., 1970, *Rev. Phys. Technol.*, **1**, 145.
3. Johnson, K.L., 1970, *J. Mech. Phys. Solids*, **18**, 115.
4. Doener, M.F., and Nix, W.D., 1986, *J. Mater. Res.*, **1**, 601.
5. Hill, R., Storakers, B., and Zdunek, A.B., 1989, *Proc. Roy. Soc. Lond.*, **A423**, 301.
6. Pharr, G.M., and Cook, R.F., 1990, *J. Mater. Res.*, **5**, 847.
7. Oliver, W.C., and Pharr, G. M., 1992, *J. Mater. Res.*, **7**, 1564.
8. Field, J.S, and Swain, M.V., 1993, *J. Mater. Res.*, **8**, 297.
9. Field, J.S, and Swain, M.V., 1995, *J. Mater. Res.*, **10**, 101.
10. Gerberich, W.W., Nelson, J.C., Lilleodden, E.T., Anderson, P., and Wyrobek, J.T., 1996, *Acta mater.*, **44**, 3585.
11. Giannakopoulos, A.E., Larsson, P.-L., and Vestergaard, R., 1994, *Int. J. Solids Structures*, **31**, 2679.
12. Larsson, P.-L., Giannakopoulos, A.E., Soderlund, E., Rowcliffe, D.J., and Vestergaard, R., 1996, *Int. J. Solids Structures*, **33**, 221.
13. Bolshakov, A., Oliver, W.C., and Pharr, G. M., 1997, *J. Mater. Res.*, **11**, 760.
14. Suresh, S., and Giannakopoulos, A.E., 1998, *Acta Mater.*, **46**, 5755.
15. Alcala, J., Giannakopoulos, A.E., and Suresh, S., 1998, *J. Mater. Res.*, **13**, 1390.
16. Cheng, Y.T., and Cheng, C.M., 1998, *J. Appl. Phys.*, **84**, 1284.
17. Cheng, Y.T., and Cheng, C.M., 1999, *J. Mater. Res.*, **14**, 3493.
18. Suresh, S., Nieh, T.-G., and Choi, B.W., 1999, *Scripta Mater.*, **41**, 951.
19. Giannakopoulos, A.E., and Suresh, S., 1999, *Scripta Mater.*, **40**, 1191.
20. Venkatesh, T.A., Van Vliet, K.J., Giannakopoulos, A.E., and Suresh, S., 2000, *Scripta Mater.*, **42**, 833.
21. Gouldstone, A., Koh, H.-J., Zeng, K.-Y., Giannakopoulos, A.E., and Suresh, S., 2000, *Acta mater.*, **48**, 2277.
22. Tunvisut, K., O'Dowd, N.P., and Busso, E.P., 2001, *Int. J. Solids Structures*, **38**, 335.
23. Dao, M., Chollacoop, N., Van Vliet, K.J., Venkatesh, T.A., and Suresh S., 2001, *Acta Mater.*, **49**, 3899.
24. Chollacoop, N., Dao, M., and Suresh S., 2003, *Acta Mater.*, **51**, 3713.
25. Bucaille, J.L., Stauss, S., Felder, E., and Michler, J., 2003, *Acta Mater.*, **51**, 1663.
26. Cao, Y.P., Lu, J., 2004, *Acta Mater.*, **52**, 1143.
27. Johnson, K.L., 1985, *Contact Mechanics*, Cambridge University Press, London.